Web of Science ™

Results: 23
(from All Databases)

You searched for: AUTHOR: (Thounthong, P.) ...**More**

Sort by: **Publication Date -- newest to oldest** Page [ ]

Select Page **Save to EndNote online** **Add to Marked List**

Create Citation Report

Refine Results

Search within results for...

Databases

Research Domains

- SCIENCE TECHNOLOGY

Refine

Research Areas

- ENGINEERING
- ENERGY FUELS
- ELECTROCHEMISTRY
- TRANSPORTATION
- TELECOMMUNICATIONS

more options / values...

Refine

Document Types

Authors

Group/Corporate Authors

Editors

Funding Agencies

Source Titles

Conference/Meeting Titles

Publication Years

Languages

Countries/Territories

1. **Performance investigation of linear and nonlinear controls for a fuel cell/supercapacitor hybrid power plant** — **Times Cited: 1** *(from All Databases)*
   By: Thounthong, Phatiphat; Tricoli, Pietro; Davat, Bernard
   INTERNATIONAL JOURNAL OF ELECTRICAL POWER & ENERGY SYSTEMS Volume: 54 Pages: 454-464 Published: JAN 2014
   View Abstract

2. **Intelligent Model-Based Control of a Standalone Photovoltaic/Fuel Cell Power Plant With Supercapacitor Energy Storage** — **Times Cited: 6** *(from All Databases)*
   By: Thounthong, Phatiphat; Luksanasakul, Arkhom; Koseeyaporn, Poolsak; et al.
   IEEE TRANSACTIONS ON SUSTAINABLE ENERGY Volume: 4 Issue: 1 Pages: 240-249 Published: JAN 2013
   View Abstract

3. **Using electrical analogy to describe mass and charge transport in PEM fuel cell** — **Times Cited: 3** *(from All Databases)*
   By: Noiying, P.; Hinaje, M.; Thounthong, P.; et al.
   RENEWABLE ENERGY Volume: 44 Pages: 128-140 Published: AUG 2012
   View Abstract

4. **Control of a Three-Level Boost Converter Based on a Differential Flatness Approach for Fuel Cell Vehicle Applications** — **Times Cited: 4** *(from All Databases)*
   By: Thounthong, Phatiphat
   IEEE TRANSACTIONS ON VEHICULAR TECHNOLOGY Volume: 61 Issue: 3 Pages: 1467-1472 Published: MAR 2012
   Full Text from Publisher **View Abstract**

5. **Model Based-Energy Control of a Solar Power Plant With a Supercapacitor for Grid-Independent Applications** — **Times Cited: 13** *(from All Databases)*
   By: Thounthong, Phatiphat
   IEEE TRANSACTIONS ON ENERGY CONVERSION Volume: 26 Issue: 4 Pages: 1210-1218 Published: DEC 2011
   Full Text from Publisher **View Abstract**

6. **Energy management of fuel cell/solar cell/supercapacitor hybrid power source** — **Times Cited: 35** *(from All Databases)*
   By: Thounthong, Phatiphat; Chunkag, Viboon; Sethakul, Panarit; et al.
   JOURNAL OF POWER SOURCES Volume: 196 Issue: 1 Special Issue: SI Pages: 313-324 Published: JAN 1 2011
   View Abstract

7. **A New Control Law Based on the Differential Flatness Principle for Multiphase Interleaved DC-DC Converter** — **Times Cited: 10** *(from All Databases)*
   By: Thounthong, Phatiphat; Pierfederici, Serge
   IEEE TRANSACTIONS ON CIRCUITS AND SYSTEMS II-EXPRESS BRIEFS Volume: 57 Issue: 11 Pages: 903-907

IEEE Xplore® DIGITAL LIBRARY

IEEE

SEARCH RESULTS

You searched for: **thounthong**

9 Results returned

Intelligent Model-Based Control of a Standalone Photovoltaic/Fuel Cell Power Plant With Supercapacitor Energy Storage

Thounthong, P. ; Luksanasakul, A. ; Koseeyaporn, P. ; Davat, B.
Sustainable Energy, IEEE Transactions on
Volume: 4 , Issue: 1
Digital Object Identifier: 10.1109/TSTE.2012.2214794
Publication Year: 2013 , Page(s): 240 - 249
Cited by: Papers (4)
IEEE JOURNALS & MAGAZINES

Differential flatness based-control of fuel cell/photovoltaic/wind turbine/supercapacitor hybrid power plant

Thounthong, P. ; Sikkabut, S. ; Mungporn, P. ; Sethakul, P. ; Pierfederici, S. ; Davat, B.
Clean Electrical Power (ICCEP), 2013 International Conference on
Digital Object Identifier: 10.1109/ICCEP.2013.6587005
Publication Year: 2013 , Page(s): 298 - 305
IEEE CONFERENCE PUBLICATIONS

Nonlinear control of a magnetic coupling converter for a supercapacitor storage device for a DC link stabilization

Thounthong, P. ; Phattanasak, M. ; Sethakul, P. ; Martin, J.-P. ; Pierfederici, S. ; Davat, B.
Clean Electrical Power (ICCEP), 2013 International Conference on
Digital Object Identifier: 10.1109/ICCEP.2013.6586954
Publication Year: 2013 , Page(s): 645 - 652
IEEE CONFERENCE PUBLICATIONS

Control strategy of solar/wind energy power plant with supercapacitor energy storage for smart DC microgrid

Sikkabut, S. ; Fuengwarodsakul, N.H. ; Sethakul, P. ; Thounthong, P. ; Pierfederici, S. ; Hinaje, M. ; Nahid-Mobarakeh, B. ; Davat, B.
Power Electronics and Drive Systems (PEDS), 2013 IEEE 10th International Conference on
Digital Object Identifier: 10.1109/PEDS.2013.6527204
Publication Year: 2013 , Page(s): 1213 - 1218
IEEE CONFERENCE PUBLICATIONS

Control of single-phase AC to DC converter for hybrid microgrid

Chunkag, C.T.V. ; Thounthong, P.
Power Electronics and Drive Systems (PEDS), 2013 IEEE 10th International Conference on
Digital Object Identifier: 10.1109/PEDS.2013.6527102
Publication Year: 2013 , Page(s): 668 - 673
IEEE CONFERENCE PUBLICATIONS

Differential flatness based control of supercapacitor substation for DC grid system

Thounthong, P. ; Sikkabut, S. ; Phattanasak, M. ; Sethakul, P. ; Pierfederici, S. ; Davat, B.
Power Electronics and Drive Systems (PEDS), 2013 IEEE 10th International Conference on
Digital Object Identifier: 10.1109/PEDS.2013.6527098
Publication Year: 2013 , Page(s): 645 - 650
IEEE CONFERENCE PUBLICATIONS

Differential flatness based control of hybrid power plant based on supercapacitor storage energy for AC distributed system

Intelligent Model-Based Control of a Standalone Photovoltaic/Fuel Cell Power Plant With Supercapacitor Energy Storage

Phatiphat Thounthong, *Member, IEEE*, Arkhom Luksanasakul, Poolsak Koseeyaporn, and Bernard Davat, *Member, IEEE*

***Abstract*—A renewable energy hybrid power plant, fed by photovoltaic (PV) and fuel cell (FC) sources with a supercapacitor (SC) storage device and suitable for distributed generation applications, is proposed herein. The PV is used as the primary source; the FC acts as a backup, feeding only the insufficiency power (steady-state) from the PV; and the SC functions as an auxiliary source and a short-term storage system for supplying the deficiency power (transient and steady-state) from the PV and the FC. For high-power applications and optimization in power converters, four-phase parallel converters are implemented for the FC converter, the PV converter, and the SC converter, respectively. A mathematical model (reduced-order model) of the FC, PV, and SC converters is described for the control of the power plant. Using the intelligent fuzzy logic controller based on the flatness property for dc grid voltage regulation, we propose a simple solution to the fast response and stabilization problems in the power system. This is the key innovative contribution of this research paper. The prototype small-scale power plant implemented was composed of a PEMFC system (1.2 kW, 46 A), a PV array (0.8 kW), and an SC module (100 F, 32 V). Experimental results validate the excellent control algorithm during load cycles.**

***Index Terms*—Flatness control, fuel cells, fuzzy control, nonlinear system, photovoltaic, supercapacitor.**

NOMENCLATURE

dc	Direct current.
FC	Fuel cell.
PV	Photovoltaic.
SC	Supercapacitor.
C_{Bus}	Total capacitance at dc bus (F).
C_{SC}	Total capacitance of supercapacitor module (F).
i_{Load}	DC bus load current (A).
i_{FC}	Fuel cell current (A).
i_{FCREF}	Fuel cell current reference (set-point) (A).
i_{PV}	Solar cell (photovoltaic) current (A).
i_{PVREF}	Solar cell current reference (set-point) (A).
i_{SC}	Supercapacitor current (A).
i_{SCREF}	Supercapacitor current reference (set-point) (A).
MPPT	Maximum power point tracking.
p_{Load}	Load power (W).
p_{FC}	Fuel cell power (W).
p_{FCo}	Fuel cell output power to dc bus (W).
p_{FCREF}	Fuel cell power reference (set-point) (W).
p_{FCMax}	Maximum fuel cell power (W).
p_{PV}	Solar cell (photovoltaic) power (W).
p_{PVo}	Solar cell output power to dc-bus (W).
p_{PVREF}	Solar cell power reference (set-point) (W).
p_{PVMax}	Maximum solar cell power (W).
p_{SC}	Supercapacitor power (W).
p_{SCo}	Supercapacitor output power to dc-bus (W).
p_{SCREF}	Supercapacitor power reference (set-point) (W).
p_{SCMax}	Maximum supercapacitor power (W).
v_{Bus}	DC bus voltage (V).
v_{FC}	Fuel cell voltage (V).
v_{PV}	Solar cell (photovoltaic) voltage (V).
v_{SC}	Supercapacitor voltage (V).
E_{Bus}	DC bus energy (J).
E_{BusREF}	DC bus energy reference (set-point) (J).
E_{SC}	Supercapacitor energy (J).
E_{SCREF}	Supercapacitor energy reference (set-point) (J).
E_T	Total energy at dc bus and supercapacitor (J).

Manuscript received December 06, 2011; revised June 13, 2012; accepted August 15, 2012. Date of publication October 02, 2012; date of current version December 12, 2012. This work was supported in part by the research program in cooperation with the Thai-French Innovation Institute (TFII), King Mongkut's University of Technology North Bangkok (KMUTNB) with Université de Lorraine, and in part by the Thailand Research Fund and Faculty of Technical Education (Research Grant for Mid-Career University Faculty) under Grant RSA5580009.

P. Thounthong. A. Luksanasakul, and P. Koseeyaporn are with the Renewable Energy Research Centre (RERC), Department of Teacher Training in Electrical Engineering, Faculty of Technical Education, King Mongkut's University of Technology North Bangkok, Bangkok 10800, Thailand (e-mail: phtt@kmutnb.ac.th; luksanasakul@gmail.com; drpoolsak@gmail.com).

B. Davat is with the Groupe de Recherche en Electrotechnique et Electronique de Nancy, Université de Lorraine, Nancy-Lorraine, France (e-mail: Bernard.Davat@ensem.inpl-nancy.fr).

Color versions of one or more of the figures in this paper are available online at http://ieeexplore.ieee.org.

Digital Object Identifier 10.1109/TSTE.2012.2214794

r_{FC}	Equivalent series resistance in fuel cell converter (Ω).
r_{PV}	Equivalent series resistance in solar cell converter (Ω).
r_{SC}	Equivalent series resistance in supercapacitor converter (Ω).
$\boldsymbol{u}$	Input variable vector.
$\boldsymbol{x}$	State-variable vector.
$\boldsymbol{y}$	Output vector.
$\phi(\cdot), \varphi(\cdot)$, and $\psi(\cdot)$	Smooth mapping functions.

I. Introduction

RENEWABLE energy sources are predicted to become competitive with conventional power generation systems in the near future. Unfortunately, they are not very reliable. For example, the PV source is not available during the night or during cloudy conditions. Other sources such as FCs may be more reliable but have economic issues associated with them. Because of this, two or more renewable energy sources are required to ensure a reliable and cost-effective power solution. Such a combination of different types of energy sources into a system is called a hybrid power system [1].

A combination of PV and FC sources forms a good pair with promising features for distributed generation applications [2]. Obviously, the slow response of the PEMFC [3], [4] needs to be compensated with a supercapacitor or a battery. A supercapacitor storage device is preferable due to its high power density, high dynamics, and long lifetime [5].

Many researchers have focused their studies on such systems. Riffonneau *et al.* [6] have studied the energy management of a grid connected PV/battery hybrid power plant. Jiang *et al.* [7] studied control based on an adaptive control with state machine estimation of an FC/Li–Ion battery hybrid power source, and Uzunoglu and Alam [8] have studied control based on a wavelet-based load sharing algorithm of an FC/SC hybrid power source.

A classical boost converter is often used as an FC converter and a PV converter [9], and a classical two-quadrant (bidirectional) converter is often used as a supercapacitor or battery converter. However, the classical converters will be limited when the power increases or at higher step-up ratios. As such, the use of parallel power converters (multiphase converters in parallel) with interleaving may offer better performance [10]. The interleaved converter can benefit both high current and high power density designs. It is ideal for merchant power applications because the reduced input ripple current and reduced output capacitor ripple current lessen the electrical stress on the dc capacitors.

Current work on controlling an FC/SC hybrid power plant is reported in [11], where a linear control using PI compensator was proposed for dc-link stabilization. Design controller parameters based on linear methods require a linear approximation [12], [13], where this is dependent on the operating point. Because the switching model of the hybrid power plant is nonlinear, it is natural to apply model-based nonlinear control strategies that directly compensate for system nonlinearity without requiring a linear approximation.

In the early 1990s, the flatness control theory was introduced by Fliess *et al.* [14] in a differential algebraic framework. It is simple, clear-cut, and appropriate for robustness, predictive control, trajectory planning, and constraints handling. Recently, this idea has been used in a variety of power electronic systems [15], [16]. Thounthong [16] has proved with real test bench results that the flatness-based control of a PV/supercapacitor power plant is absolutely robust.

The fast response, efficiency, and stability of the operation of hybrid power plants are of particular interest. In this work, a hybrid power generation system is studied, consisting of the following main components: a PV, proton exchange membrane FCs (PEMFC), and an SC as a high-power density device. In this study, a novel framework is proposed for the intelligent fuzzy logic-based flatness control approach of a solar-hydrogen power generation system with a supercapacitor storage device. The rest of the paper is structured as follows: Section II describes the hybrid energy system and modeling of the power plant that is studied in this work. Section III presents the proposed energy management algorithm, the proof of the flat system of the renewable energy power plant, and the control laws and system stability. Section IV presents test bench results for the proposed system. Finally, the paper ends with concluding remarks in Section V.

II. Solar/Hydrogen Power Plant

A. Structure of Power Converters Studied

The power converter structure of the system studied in this paper is shown in Fig. 1. The FC and PV converters have four-phase parallel boost converters and the SC converter has four-phase parallel bidirectional converters (two-quadrant converters). For optimization in power converters, these converters connected in parallel, with an *interleaved switching technique*, increase the power processing capability and availability of the power electronic system [10].

For safety and high dynamics, the PV, FC, and SC converters are primarily controlled by inner current regulation loops classically. To ensure system stability, the dynamics of the inner regulation loops are also supposed to be much faster than those of the outer control loops [13]. These current control loops are supplied by three reference signals: i_{SCREF}, i_{PVREF}, and i_{FCREF}, generated by the control laws, presented hereafter.

B. Mathematical Model of the Power Plant

We consider that the PV, FC, and SC currents follow their reference values perfectly. This is a classical assumption used in the cascade control structure in order to estimate the external control loop. However, the assumption error will be compensated by the intelligent external control loop. Then, the inner control loops of the PV, FC, and SC powers can be approximated as a unity gain. The PV power reference p_{PVREF}, the FC

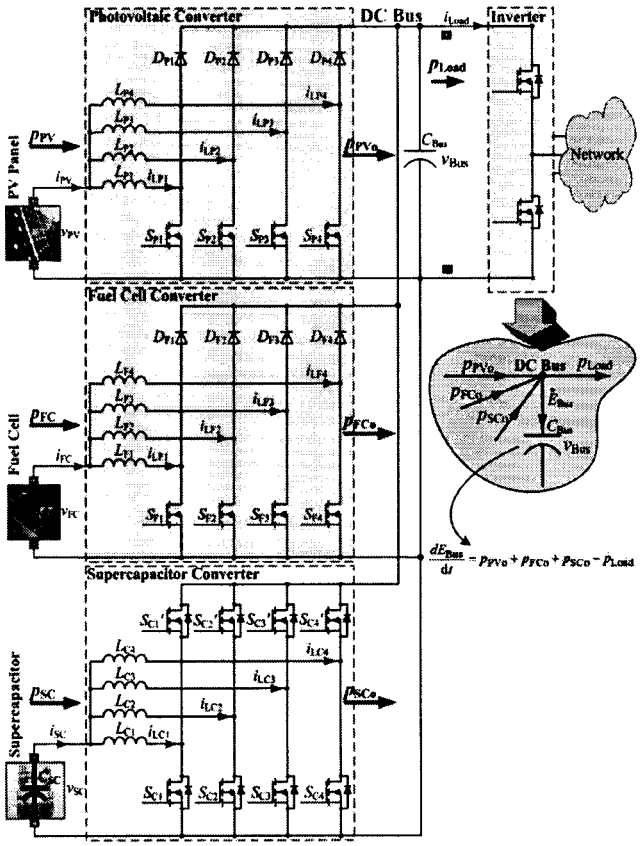

Fig. 1. Proposed circuit diagram of power plant supplied by an FC, a PV, and SC.

power reference p_{FCREF}, and the SC power reference p_{SCREF} are

$$p_{\mathrm{PVREF}} = p_{\mathrm{PV}} = v_{\mathrm{PV}} \cdot i_{\mathrm{PV}} \tag{1}$$

$$p_{\mathrm{FCREF}} = p_{\mathrm{FC}} = v_{\mathrm{FC}} \cdot i_{\mathrm{FC}} \tag{2}$$

$$p_{\mathrm{SCREF}} = p_{\mathrm{SC}} = v_{\mathrm{SC}} \cdot i_{\mathrm{SC}}. \tag{3}$$

The PV panel, the FC generator, and the SC storage device function as controlled power sources. We assume here that there are only static losses in these converters, in which r_{PV}, r_{FC}, and r_{SC} represent the only static losses in the PV, the FC, and the SC converters, respectively. In real environment, the losses in converters are varied depending on many factors: temperature, current flow, etc. However, the estimation error will be compensated by the intelligent controller, presented hereafter. So, the dc-bus capacitive energy E_{Bus} and the supercapacitive energy E_{SC} can be written as

$$E_{\mathrm{Bus}} = \frac{1}{2} C_{\mathrm{Bus}} v_{\mathrm{Bus}}^2, \quad E_{\mathrm{SC}} = \frac{1}{2} C_{\mathrm{SC}} v_{\mathrm{SC}}^2. \tag{4}$$

The total electrostatic energy E_T stored in the dc-bus capacitor C_{Bus} and in the supercapacitor C_{SC} can also be written as

$$E_T = \frac{1}{2} C_{\mathrm{Bus}} v_{\mathrm{Bus}}^2 + \frac{1}{2} C_{\mathrm{SC}} v_{\mathrm{SC}}^2. \tag{5}$$

As portrayed in Fig. 1, the derivative of dc-bus capacitive energy E_{Bus} is given versus $p_{\mathrm{PVo}}, p_{\mathrm{FCo}}, p_{\mathrm{SCo}}$, and p_{Load} by the following differential equation:

$$\dot{E}_{\mathrm{Bus}} = p_{\mathrm{PVo}} + p_{\mathrm{FCo}} + p_{\mathrm{SCo}} - p_{\mathrm{Load}} \tag{6}$$

where

$$p_{\mathrm{PVo}} = p_{\mathrm{PV}} - r_{\mathrm{PV}} \left(\frac{p_{\mathrm{PV}}}{v_{\mathrm{PV}}} \right)^2 \tag{7}$$

$$p_{\mathrm{FCo}} = p_{\mathrm{FC}} - r_{\mathrm{FC}} \left(\frac{p_{\mathrm{FC}}}{v_{\mathrm{FC}}} \right)^2 \tag{8}$$

$$p_{\mathrm{SCo}} = p_{\mathrm{SC}} - r_{\mathrm{SC}} \left(\frac{p_{\mathrm{SC}}}{v_{\mathrm{SC}}} \right)^2 \tag{9}$$

$$p_{\mathrm{Load}} = v_{\mathrm{Bus}} \cdot i_{\mathrm{Load}} = \sqrt{\frac{2E_{\mathrm{Bus}}}{C_{\mathrm{Bus}}}} \cdot i_{\mathrm{Load}} \tag{10}$$

$$p_{\mathrm{SC}} = v_{\mathrm{SC}} \cdot i_{\mathrm{SC}} = \sqrt{\frac{2E_{\mathrm{SC}}}{C_{\mathrm{SC}}}} \cdot i_{\mathrm{SC}}. \tag{11}$$

III. Nonlinear Model-Based Control of a Power Plant

A. Energy Balance

The main control objectives are stability, high overall efficiency, and fast response. As for supplying energy to the load demanded and the charging storage device, the multivariable control here involves set-point control of the dc-bus voltage v_{Bus} (representing the dc-bus energy E_{Bus}, called "*DC link stabilization*") [11] and set-point control of the SC voltage v_{SC} (representing the supercapacitive energy E_{SC}).

The principle behind the proposed hybrid energy management lies in using the SCs (the fastest energy source) to supply the energy required to achieve the dc grid voltage regulation (or the dc bus energy regulation) [11]. Then, the PV and FC, although clearly the main energy source of the system, function as the generator that supplies energy for both the dc bus capacitor C_{Bus} and the C_{SC} to keep them charged.

B. Flatness of the Power Plant Model

For the substantiation of flatness [17], [18], the system explanation from Section II is examined. To regulate the dc-bus voltage v_{Bus} (DC link stabilization) and the SC voltage v_{SC} (state-of-charge), based on the flatness control theory introduced above, the flat outputs $\boldsymbol{y}$, the control input variables $\boldsymbol{u}$, and the state variables $\boldsymbol{x}$ are defined as

$$\mathbf{y} = \begin{bmatrix} y_1 \\ y_2 \end{bmatrix} = \begin{bmatrix} E_{\mathrm{Bus}} \\ E_T \end{bmatrix}, \quad \mathbf{u} = \begin{bmatrix} u_1 \\ u_2 \end{bmatrix} = \begin{bmatrix} p_{\mathrm{SCREF}} \\ p_{\mathrm{TREF}} \end{bmatrix}$$
$$\mathbf{x} = \begin{bmatrix} x_1 \\ x_2 \end{bmatrix} = \begin{bmatrix} v_{\mathrm{Bus}} \\ v_{\mathrm{SC}} \end{bmatrix} \tag{12}$$

where p_{TREF} is the total power from the FC and PV array. From (4) and (5), the state variables $\boldsymbol{x}$ can be written as

$$x = \begin{bmatrix} x_1 \\ x_2 \end{bmatrix} = \begin{bmatrix} \sqrt{\frac{2y_1}{C_{\mathrm{Bus}}}} \\ \sqrt{\frac{2(y_2 - y_1)}{C_{\mathrm{SC}}}} \end{bmatrix} = \begin{bmatrix} \varphi_1(y_1) \\ \varphi_2(y_1, y_2) \end{bmatrix}. \tag{13}$$

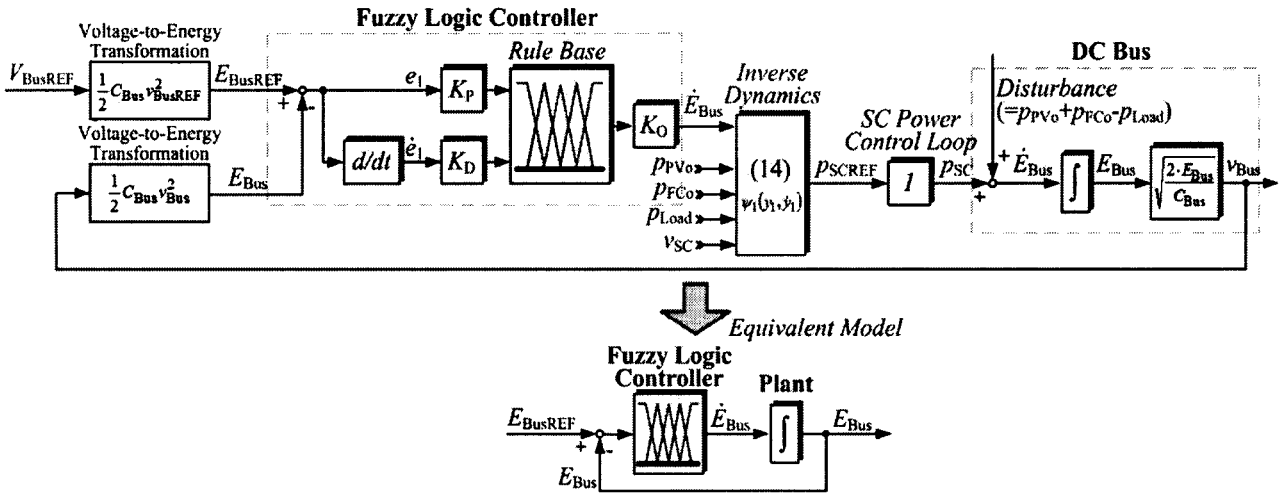

Fig. 2. Control law based on the differential flatness theory of the dc-bus energy regulation for PV/FC/SC hybrid power plant.

From (6) to (11), the control input variables $\boldsymbol{u}$ can be calculated from the flat output $\boldsymbol{y}$ and its time derivatives

$$u_1 = 2p_{\mathrm{SCLim}} \cdot \left[1 - \sqrt{1 - \left(\frac{\dot{y}_1 + \sqrt{\frac{2y_1}{C_{\mathrm{Bus}}}} \cdot i_{\mathrm{Load}} - p_{\mathrm{FCo}} - p_{\mathrm{PVo}}}{p_{\mathrm{SCLim}}}\right)}\right] = \psi_1(y_1, \dot{y}_1) \tag{14}$$

$$u_2 = 2p_{\mathrm{TMax}} \cdot \left[1 - \sqrt{1 - \left(\frac{\dot{y}_2 + \sqrt{\frac{2y_1}{C_{\mathrm{Bus}}}} \cdot i_{\mathrm{Load}}}{p_{\mathrm{TMax}}}\right)}\right] = \psi_2(y_1, \dot{y}_2) \tag{15}$$

where

$$p_{\mathrm{SCLim}} = \frac{v_{\mathrm{SC}}^2}{4r_{\mathrm{SC}}}, \quad p_{\mathrm{TMax}} = \frac{v_T^2}{4r_T}. \tag{16}$$

p_{SCLim} is the limited maximum power from the SC converter, v_T is the virtual voltage from the FC and PV power generators, and r_T is the virtual static losses in the FC and PV power converters.

In fact,

$$p_{\mathrm{TMax}} = p_{\mathrm{FCMax}} + p_{\mathrm{PVMax}} \tag{17}$$

where p_{FCMax} is the maximum FC power and p_{PVMax} is the maximum PV power.

Thus, it is understandable that $x_1 = \varphi_1(y_1), x_2 = \varphi_2(y_1, y_2), u_1 = \psi_1(y_1, \dot{y}_1)$, and $u_2 = \psi_2(y_1, \dot{y}_2)$. The proposed reduced order model can be studied as a flat system [17], [18].

C. DC Link Stabilization

Fuzzy control algorithms offer many advantages over traditional controls because they give fast convergence, are parameter insensitive, and accept noisy and inaccurate signals [19], [20]. In recent years, it has been used in many control applications where the system is complex [21], [22].

The control objective is to regulate the dc bus voltage v_{Bus} or the dc bus energy $E_{\mathrm{Bus}}(= y_1)$. The controller contains a Takagi–Sugeno (T-S) inference engine and two fuzzy inputs: the energy error $e_1(= y_{1\mathrm{REF}} - y_1)$ and the differential energy error $\dot{e}_1$, which are carefully adjusted using the proportional gain K_P and the derivative gain K_D, respectively. In addition, the fuzzy output level can be set by the proportional gain K_O (Fig. 2).

Triangular and trapezoidal membership functions are chosen for both of the fuzzy inputs, as shown in Fig. 3(a). There are seven membership functions for each input, including NB (Negative Big), NM (Negative Medium), NS (Negative Small), Z (Zero), PB (Positive Big), PM (Positive Medium), and PS (Positive Small). For the singleton output membership function, the zero-order Sugeno model is used, where the membership functions are specified symmetrically, as follows: $NB = -1$, $NM = -0.66$, $NS = -0.33$, $Z = 0$, $PB = 1$, $PM = 0.66$, and $PS = 0.33$, as presented in Fig. 3(b).

For the rule base, expert suggestions, an experimental approach, and a trial and error technique were used to define the relationships between the inputs and the output. The data representation was in the form of an *IF-THEN* rule, as shown in the following example:

```
IF e1i is NS and ė1i is NS
        THEN zi(=output) is NB.
```

As shown in Fig. 3(c), the total number of rule bases is, therefore, equal to 49 rules. To obtain the output of the controller, the center of gravity method for the *COGS* of the singletons is utilized as

$$U = \frac{\sum_{i=1}^{N} w_i z_i}{\sum_{i=1}^{N} w_i} \tag{18}$$

where the weights (w_i) can be retrieved from

$$w_i = \mathbf{max}(e_{1i}, \dot{e}_{1i}). \tag{19}$$

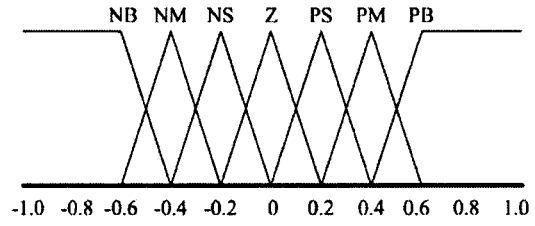

(a)

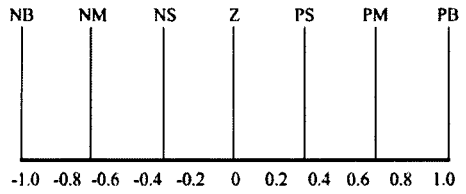

(b)

$\dot{e}/e$	NB	NM	NS	Z	PS	PM	PB
NB	PB	PB	PB	PB	PB	PB	PM
NM	PB	PB	PB	PM	PM	PM	PM
NS	PM	PM	PM	PS	PS	Z	Z
Z	PB	PM	PS	Z	NS	NM	NB
PS	Z	Z	NS	NS	NM	NM	NM
PM	NM	NM	NM	NM	NB	NB	NB
PB	NM	NB	NB	NB	NB	NB	NB

(c)

Fig. 3. Rule base and membership functions. (a) Input membership functions. (b) Output membership function. (c) Rule base.

D. Charging Supercapacitor

Because the SC energy storage has a massive size capacity, and the supercapacitive energy is defined as a slower dynamic variable than the dc-bus energy variable. Then, the proposed control law is [23], [24]

$$(\dot{y}_2 - \dot{y}_{2\mathrm{REF}}) + K_{21}(y_2 - y_{2\mathrm{REF}}) = 0. \tag{20}$$

This yields

$$\dot{y}_2 = \dot{y}_{2\mathrm{REF}} + K_{21}(y_{2\mathrm{REF}} - y_2) \tag{21}$$

where $y_{2\mathrm{REF}}$ is the reference of total electrostatic energy, refer to (5), and K_{21} is the control parameter.

From (20), if we define $e_2 = y_2 - y_{2\mathrm{REF}}, K_{21} = 1/\tau_S$, we obtain

$$\tau_S \cdot \dot{e}_2 + e_2 = 0. \tag{22}$$

Substituting the expression for $\dot{y}_2$ from (21) into (15) gives the equation for the closed-loop static state feedback, in which one obtains the inverse dynamics

$$\begin{aligned} u_2 &= \psi_2(y_1, \dot{y}_2) = p_{\mathrm{TREF}} \\ &= p_{\mathrm{PVDEM}} + p_{\mathrm{FCDEM}} \end{aligned} \tag{23}$$

where p_{PVDEM} is the PV power demand and p_{FCDEM} is the FC power demand.

The total energy control law (or the SC energy control law) generates a total power reference p_{TREF}, as shown in Fig. 4. First, p_{TREF} is considered as the PV power demand p_{PVDEM}. It must be limited in level, within an interval maximum p_{PVMax} (maximum power point tracking MPPT) and minimum p_{PVMin} (set to 0 W). Several approaches have been devised for tracking MPP accurately for PV cells [25], [26]. Some of the popular ones are the perturbation and observation algorithm (P&O) method [27]. Based on P&O MPPT, the pseudocode for the PV power saturation function studied here is described in ALGORITHM I, where ΔI_{PV} is the defined PV current step size and Δt_{PV} is the sampling time. Note that this sampling time must be higher than a main program sampling time.

ALGORITHM I: MPPT for PV

BEGIN

READ $p_{\mathrm{PVDEM}}(t)$

READ $v_{\mathrm{PV}}(t)$

READ $i_{\mathrm{PV}}(t)$

$p_{\mathrm{PV}}(t) = v_{\mathrm{PV}}(t) \times i_{\mathrm{PV}}(t)$

$p_{\mathrm{PV}}(t - \Delta t_{\mathrm{PV}}) = v_{\mathrm{PV}}(t - \Delta t_{\mathrm{PV}}) \times i_{\mathrm{PV}}(t - \Delta t_{\mathrm{PV}})$

IF $p_{\mathrm{PV}}(t) \geq p_{\mathrm{PV}}(t - \Delta t_{\mathrm{PV}})$ **THEN**

IF $i_{\mathrm{PV}}(t) \geq i_{\mathrm{PV}}(t - \Delta t_{\mathrm{PV}})$ **THEN**

$i_{\mathrm{PVMax}}(t) = i_{\mathrm{PV}}(t) + \Delta I_{\mathrm{PV}}$

ELSE

$i_{\mathrm{PVMax}}(t) = i_{\mathrm{PV}}(t) - \Delta I_{\mathrm{PV}}$

ELSEIF

ELSE

IF $i_{\mathrm{PV}}(t) \geq i_{\mathrm{PV}}(t - \Delta t_{\mathrm{PV}})$ **THEN**

$i_{\mathrm{PVMax}}(t) = i_{\mathrm{PV}}(t) - \Delta I_{\mathrm{PV}}$

ELSE

$i_{\mathrm{PVMax}}(t) = i_{\mathrm{PV}}(t) + \Delta I_{\mathrm{PV}}$

ELSEIF

ENDIF

$p_{\mathrm{PVMax}}(t) = v_{\mathrm{PV}}(t) \times i_{\mathrm{PVMax}}(t)$

$p_{\mathrm{PVREF}}(t) = \mathbf{min}[p_{\mathrm{PVDEM}}(t), p_{\mathrm{PVMax}}(t)]$

$v_{\mathrm{PV}}(t - \Delta t_{\mathrm{PV}}) = v_{\mathrm{PV}}(t)$

$i_{\mathrm{PV}}(t - \Delta t_{\mathrm{PV}}) = i_{\mathrm{PV}}(t)$

END

Second, the difference between the total power reference p_{TREF} and the PV power reference p_{PVREF} is the FC power demand p_{FCDEM}. It must be limited in level, within an interval maximum p_{FCMax} and minimum p_{FCMin} (set to 0 W) and limited in dynamics to respect the constraints that are associated

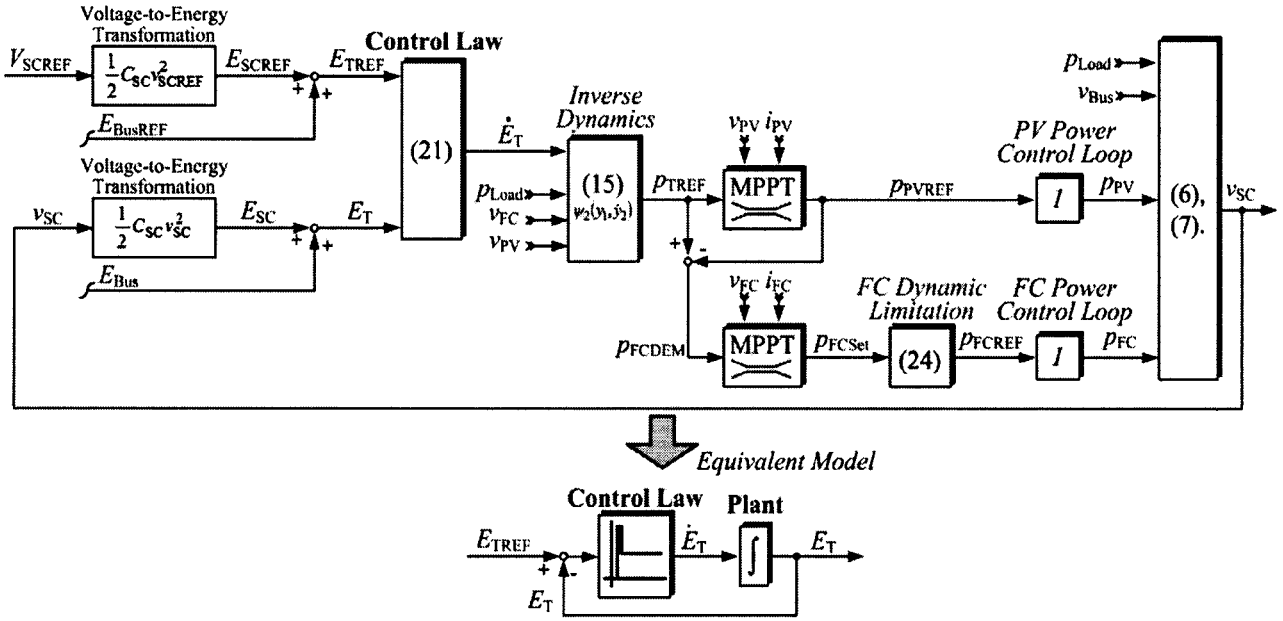

Fig. 4. Control law of the total energy regulation (charging supercapacitor) for PV/FC/SC hybrid power plant.

with the FC [4]. Based on P&O MPPT, the pseudocode for the FC power saturation function is similar to ALGORITHM I.

The typical polarization curve of a PEMFC is dependent on many factors: temperature, humidity, cell current, etc., [28], [29]. Moreover, the lifetime target requires PEMFCs to achieve 5000 h for mobile and 40 000 h for stationary applications. Normal degradation targets require less than 10% loss in the efficiency of the fuel cell system at the end of life, and a degradation rate of 2–10 μV·h^{-1} [30], [31]. For these reasons, the MPPT for FC is obligatory. So, to limit the transient FC power [32], [33], a low-pass filter (second order) is employed such that the power demand p_{FCSet} from MPPT is always limited by

$$p_{\mathrm{FCREF}}(t) = p_{\mathrm{FCSet}}(t) \cdot \left(1 - e^{-\frac{t}{\tau_1}} - \frac{t}{\tau_1} e^{-\frac{t}{\tau_1}}\right) \quad (24)$$

where τ_1 is the control parameter.

IV. Performance Validations

A. Test Bench Description

To authenticate the performance of the modeling and control system, a test bench was implemented. The small-scale test bench of the renewable power plant was implemented in our laboratory, as presented in Fig. 5. The prototype FC converter of 1 kW, the PV converter of 0.8 kW, and the SC converter of 2 kW (refer to Fig. 1) were realized in the laboratory. Specifications of the real power sources and storage device are detailed in Table I. Note that the PV panel is installed on the roof of the laboratory building (Fig. 5). It means that the PV energy production is directly from the sun.

The efficiency of each converter is around 85%, because the implemented converters are hard-switching converters. So, the power losses can be observed in the following experimental results. To improve the converter efficiency, soft-switching converters may be effective solutions for future work.

B. Control Description

The parameters associated with the dc-bus energy regulation loop are summarized in Table II. Note that K_O fuzzy logic controller is negative value because of the membership function and rule base as presented in Fig. 3. Parameters associated with the SC energy regulation loop are detailed in Table III. The FC, PV, and SC current regulation loops were realized by analog circuits. The two energy control loops, which generate current references i_{FCREF}, i_{PVREF} and i_{SCREF}, were implemented in the real time card dSPACE DS1104 (see Fig. 5), through the mathematical environment of Matlab-Simulink, with a sampling frequency of 25 kHz.

C. Experimental Results

Fig. 6 presents waveforms that are obtained during the long load cycles measured on March 29, 2011. The experimental tests were carried out by connecting a dc link loaded by an electronic load. The load will be varied in order to emulate the real environment: light load, over load, positive transition (↑), and negative transition (↓). The data show the dc bus voltage, the FC voltage, the load power, the SC power, the FC power, the PV power, the SC current, the FC current, the PV current, and the SC voltage. In the initial state, the small load power is equal to 280 W, and the SC storage device is full of charge, i.e., $v_{\mathrm{SC}} = V_{\mathrm{SCNom}} = V_{\mathrm{SCREF}} = 25$ V; as a result, the photovoltaic source supplies power for the load of 280 W (because $p_{\mathrm{PVMax}} > p_{\mathrm{PVDEM}}$, then $p_{\mathrm{PVREF}} = p_{\mathrm{PVDEM}}$), and the FC and SC powers are zero.

At 9:00:50, the large load power steps from 280 W to the final constant power of 900 W (positive load power transition). The following observations are made:

1) The SC supplies most of the transient step load.
2) Concurrently, the photovoltaic power increases to a maximum power point (MPP) of around 350 W, which is limited by the maximum power point tracker (MPPT), because $p_{\mathrm{PVMax}} < p_{\mathrm{PVDEM}}$, then $p_{\mathrm{PVREF}} = p_{\mathrm{PVMax}}$.

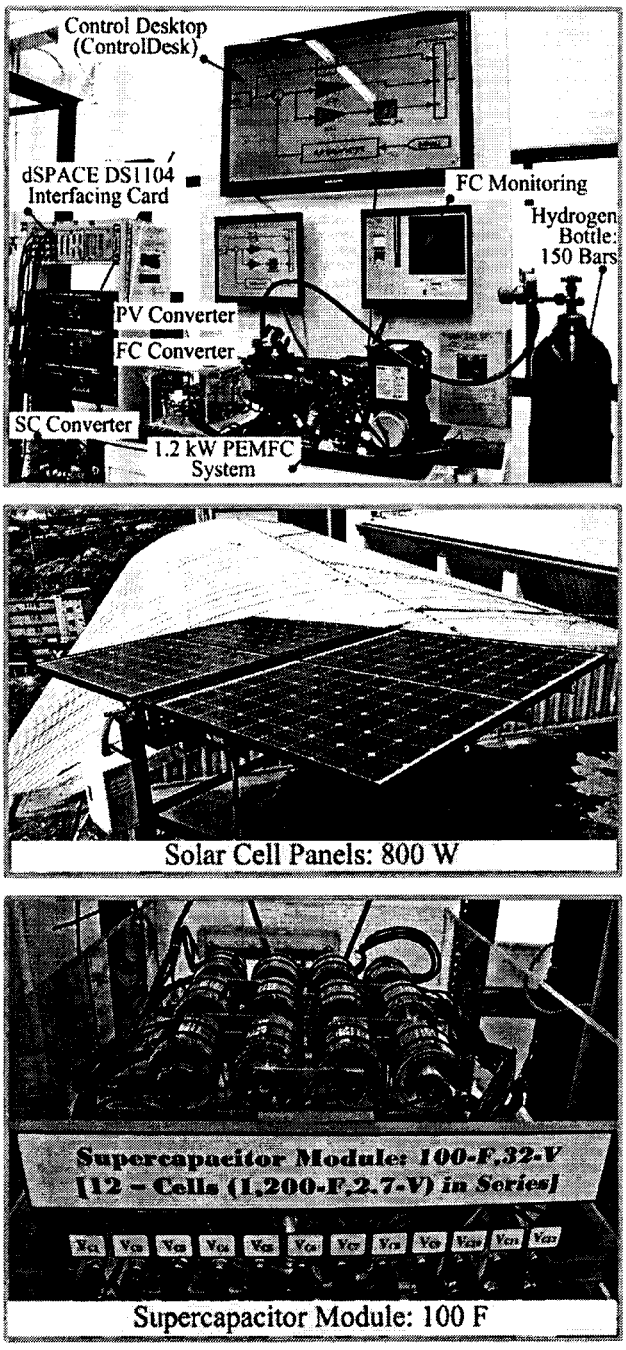

Fig. 5. Photograph of the experimental setup.

3) At the same time, the FC power increases with limited dynamics to MPP of around 430 W.
4) The input from the SC, which supplies most of the transient power that is required during the stepped load, slowly decreases and the unit remains in a discharge state after the load step because the steady-state load power (approximately 900 W) is greater than the total power supplied by the photovoltaic array and fuel cell. This state is known as the ride-through mode.

After that, at 9:02:10, the load power steps from 900 to 280 W (negative transition) and $V_{\mathrm{SCREF}}(= 25\ \mathrm{V}) > v_{\mathrm{SC}}(= 17\ \mathrm{V})$. As a result, the SC changes its state from discharging to charging, demonstrating the four phases.

TABLE I
SPECIFICATIONS OF POWER SOURCES AND STORAGE DEVICE

Fuel Cell System (by Ballard Power Systems Inc):		
Rated Power	1,200	W
Rated Current	46	A
Rated Voltage	26	V
Photovoltaic Array (by Ekarat Solar Company):		
Number of Panels in Parallel	4	
Panel Open Circuit Voltage	33.5	V
Panel Rated Voltage	26	V
Panel Rated Current	7.7	A
Panel Rated Power	200	W
Array Rated Power	800	W
Supercapacitor Bank (by Maxwell Technologies Comp): (Cell Model: BCAP1200)		
Number of Cells in Series	12	
Cell Capacity	1,200	F
Cell Maximum Voltage	2.7	V
Bank Capacity (C_{SC})	100	F
Bank Maximum Voltage	32	V

TABLE II
DC-BUS ENERGY CONTROL LOOP PARAMETERS

V_{BusREF}	60	V
C_{Bus}	12200	μF
K_{P}	0.15	
K_{D}	0.15	
K_{O}	−200	
r_{PV}	0.13	Ω
r_{FC}	0.13	Ω
r_{SC}	0.08	Ω
V_{SCMax}	32	V
V_{SCMin}	15	V
I_{SCRated}	150	A

TABLE III
SUPERCAPACITIVE ENERGY CONTROL LOOP PARAMETERS

V_{SCREF}	25	V
C_{SC}	100	F
K_{21}	0.1	$\mathrm{W{\cdot}J^{-1}}$
p_{FCMin}	0	W
I_{FCMax} (Rated)	46	A
I_{FCMin}	0	A
τ_{I}	5	s

1) First, the FC and PV still supply their total limited maximum powers for driving the load and for charging the SC, intelligently.
2) Second, at 9:02:35 ($v_{\mathrm{SC}} = 23.5$ V), the SC is nearly charged at 25 V; which then reduces the charging power. As a result, the FC power is reduced to zero.
3) Third, at 9:03:00 ($v_{\mathrm{SC}} = 24.5$ V), the SC is nearly fully charged at 25 V; as a result, the PV power is reduced.
4) Fourth, at 9:03:20, the SC is fully charged ($V_{\mathrm{SCREF}} = v_{\mathrm{SC}} = 25.0$ V). As a result, the FC and SC powers are zero; the PV source supplies power for the load of 280 W.

During the experiment, the FC maximum power is limited by the MPPT and the PV maximum power is limited by the MPPT. Exceptionally, one can observe that the power plant is always energy balanced ($p_{\mathrm{Load}} = p_{\mathrm{PV}} + p_{\mathrm{FC}} + p_{\mathrm{SC}}$) by the proposed original control algorithm.

The oscilloscope waveforms in Fig. 7 show the dynamic response of the dc bus voltage dynamics to the large load power

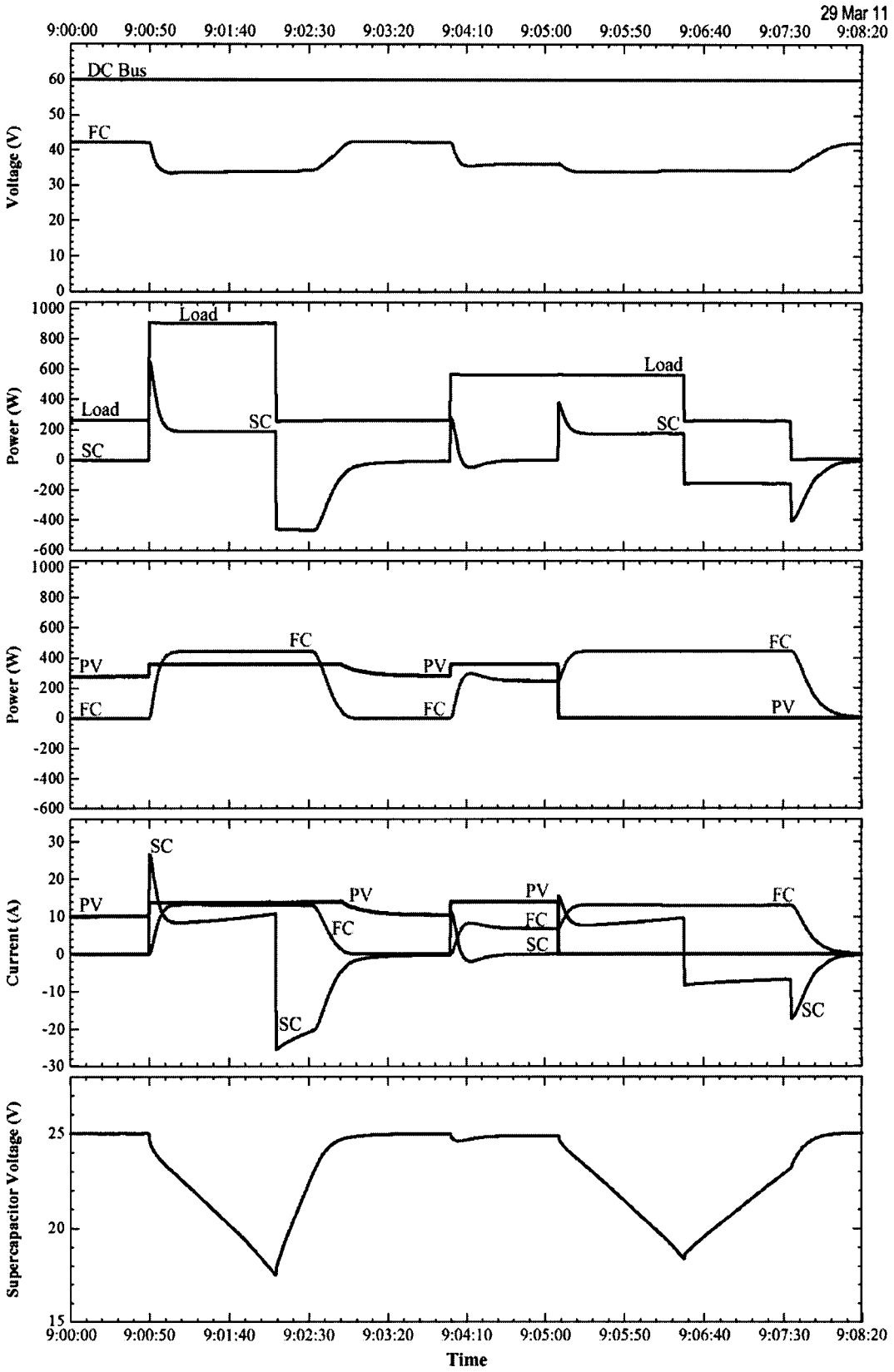

Fig. 6. Experimental results: Power plant response during load cycles.

demands (disturbance) from 0 to 900 W. The oscilloscope screens show the dc bus voltage, the SC voltage, the load power, and the SC power. The PV and FC power dynamics were purposely limited, forcing the SC to supply the transient load power demand. The proposed fuzzy-logic controller shows good stability and an optimum response (no oscillation and short settling time) for the regulation of the dc bus voltage to the desired reference of 60 V.

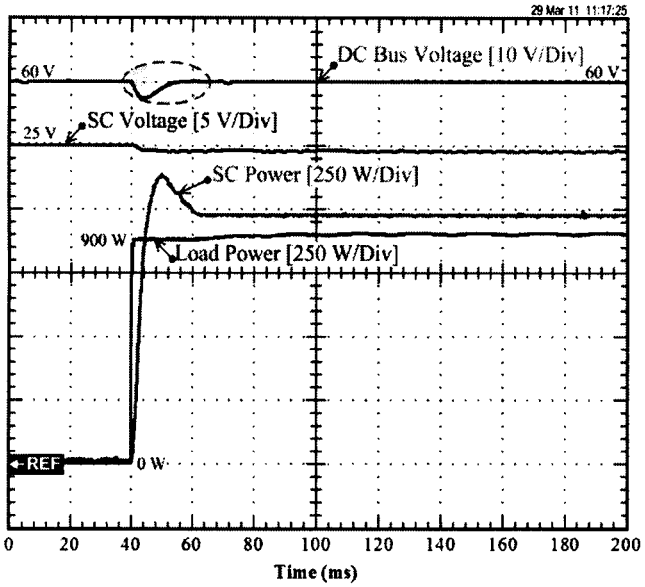

Fig. 7. Experimental results of the dynamic characteristics of the power plant during a step load from 0 to 900 W.

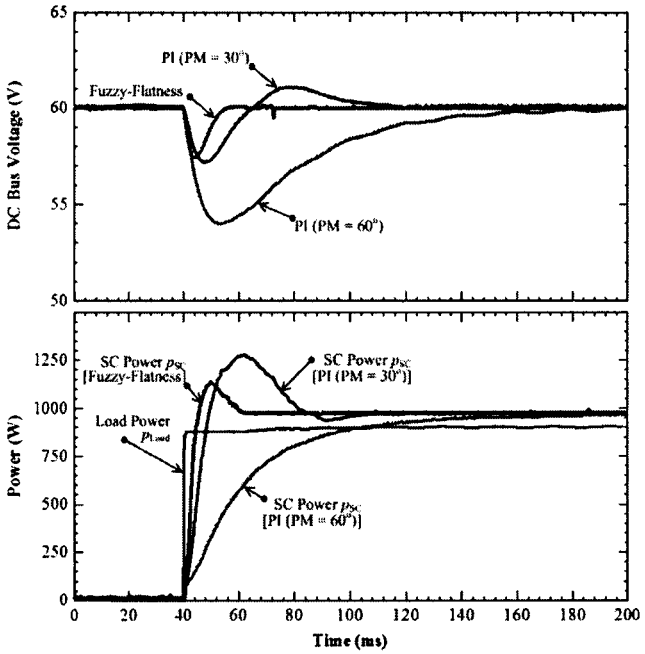

Fig. 8. Comparison of the fuzzy-flatness based control law with a linear PI control law during a large load step.

Finally, to compare the performance of the proposed control law, a traditional linear PI control method presented in [11] was also implemented on the test bench. In order to give a rational comparison between the methods, the parameters of the linear controller K_P and K_I were tuned to obtain the best possible performance. The desired phase margin (PM) was tuned at 30° and 60°. This result was compared to the fuzzy-flatness-based control. Fig. 8 shows experimental results obtained for both controllers during the large load step. The fuzzy-flatness-based control shows good stability and optimum response of the dc-bus voltage regulation to its desired reference of 60 V. Although dynamic response of the linear control law could be improved relative to that shown in the figures, this enhancement comes at the expense of a reduced stability margin (overshoot and oscillation). From these results, we conclude that fuzzy-flatness-based control provides better performance than the classical PI controller.

V. Conclusion

The key contribution of this paper is to authenticate the intelligent fuzzy logic control based on differential flatness estimation of a PV/FC/SC hybrid power plant for standalone applications. The prototype power plant studied was composed of a PEMFC system (1200 W), a PV array (800 W), and an SC module (100 F). Its working principle, analysis, and design procedure were presented. The PV is the main source, while the FC serves as a support source to compensate for the uncertainties of the PV source in the steady state. The SC functions as a storage device (or an auxiliary source) to compensate for the uncertainties of the PV and FC sources in the steady state and transient state.

Using the intelligent fuzzy logic control for dc link stabilization based on the flatness property, we proposed simple solution to the fast response and stabilization problems in the nonlinear power electronic system. This strategy is based on a standard dc link voltage regulation, which is simpler than standard state machines used for hybrid source control, and free of chattering problems. This is the novel concept for this kind of application. Experimental results authenticated the control algorithm and control laws.

Acknowledgment

The authors would like to thank Dr. P. Sethakul (KMUTNB) and Dr. S. Pierfederici (Université de Lorraine) for their valuable comments and suggestions about power electronics and control.

References

[1] M. H. Nehrir, C. Wang, K. Strunz, H. Aki, R. Ramakumar, J. Bing, Z. Miao, and Z. Salameh, "A review of hybrid renewable/alternative energy systems for electric power generation: Configurations, control, and applications," *IEEE Trans. Sustain. Energy*, vol. 2, no. 4, pp. 392–403, Oct. 2011.

[2] P. Thounthong, V. Chunkag, P. Sethakul, S. Sikkabut, S. Pierfederici, and B. Davat, "Energy management of fuel cell/solar cell/supercapacitor hybrid power source," *J. Power Sources*, vol. 196, no. 1, pp. 313–324, Jan. 2011.

[3] A. Ravey, N. Watrin, B. Blunier, D. Bouquain, and A. Miraoui, "Energy-source-sizing methodology for hybrid fuel cell vehicles based on statistical description of driving cycles," *IEEE Trans. Veh. Technol.*, vol. 60, no. 9, pp. 4164–4174, Nov. 2011.

[4] T. Azib, O. Bethoux, G. Remy, and C. Marchand, "Saturation management of a controlled fuel-cell/ultracapacitor hybrid vehicle," *IEEE Trans. Veh. Technol.*, vol. 60, no. 9, pp. 4127–4138, Nov. 2011.

[5] A. S. Weddell, G. V. Merrett, T. J. Kazmierski, and B. M. Al-Hashimi, "Accurate supercapacitor modeling for energy harvesting wireless sensor nodes," *IEEE Trans. Circuits Syst. II, Exp. Brief*, vol. 58, no. 12, pp. 911–915, Dec. 2011.

[6] Y. Riffonneau, S. Bacha, F. Barruel, and S. Ploix, "Optimal power flow management for grid connected PV systems with batteries," *IEEE Trans. Sustain. Energy*, vol. 2, no. 3, pp. 309–420, Jul. 2011.

[7] Z. Jiang, L. Gao, and R. A. Dougal, "Adaptive control strategy for active power sharing in hybrid fuel cell/battery power sources," *IEEE Trans. Energy Convers.*, vol. 22, no. 2, pp. 507–515, Jun. 2007.

[8] M. Uzunoglu and M. S. Alam, "Modeling and analysis of an FC/UC hybrid vehicular power system using a novel-wavelet-based load sharing algorithm," *IEEE Trans. Energy Convers.*, vol. 23, no. 1, pp. 263–272, Mar. 2008.

[9] W. Na, T. Park, T. Kim, and S. Kwak, "Light fuel-cell hybrid electric vehicles based on predictive controllers," *IEEE Trans. Veh. Technol.*, vol. 60, no. 1, pp. 89–97, Jan. 2011.
[10] P. Thounthong and S. Pierfederici, "A new control law based on the differential flatness principle for multiphase interleaved DC-DC converter," *IEEE Trans. Circuits Syst. II, Exp. Briefs*, vol. 57, no. 11, pp. 903–907, Nov. 2010.
[11] P. Thounthong, S. Raël, and B. Davat, "Control strategy of fuel cell and supercapacitors association for distributed generation system," *IEEE Trans. Ind. Electron.*, vol. 54, no. 6, pp. 3225–3233, Dec. 2007.
[12] C. Xia, X. Gu, T. Shi, and Y. Yan, "Neutral-point potential balancing of three-level inverters in direct-driven wind energy conversion system," *IEEE Trans. Energy Convers.*, vol. 26, no. 1, pp. 18–29, Mar. 2011.
[13] H. Zhou, G. Yang, and J. Wang, "Modeling, analysis, and control for the rectifier of hybrid HVdc systems for DFIG-based wind farms," *IEEE Trans. Energy Convers.*, vol. 26, no. 1, pp. 340–353, Mar. 2011.
[14] M. Fliess, J. Levine, Ph. Martin, and P. Rouchon, "A Lie-Bäcklund approach to equivalence and flatness of nonlinear systems," *IEEE Trans. Automat. Contr.*, vol. 44, no. 5, pp. 922–937, May 1999.
[15] M. Zandi, A. Payman, J.-Ph. Martin, S. Pierfederici, B. Davat, and F. Meibody-Tabar, "Energy management of a fuel cell/supercapacitor/battery power source for electric vehicular applications," *IEEE Trans. Veh. Technol.*, vol. 60, no. 2, pp. 433–443, Feb. 2011.
[16] P. Thounthong, "Model based-energy control of a solar power plant with a supercapacitor for grid-independent applications," *IEEE Trans. Energy Convers.*, vol. 26, no. 4, pp. 1210–1218, Dec. 2011.
[17] A. Gensior, T. M. P. Nguyen, J. Rudolph, and H. Güldner, "Flatness-based loss optimization and control of a doubly fed induction generator system," *IEEE Trans. Control Syst. Technol.*, vol. 19, no. 6, pp. 1457–1466, Nov. 2011.
[18] C. P. Tang, P. T. Miller, V. N. Krovi, J.-C. Ryu, and S. K. Agrawal, "Differential-flatness-based planning and control of a wheeled mobile manipulator—Theory and experiment," *IEEE/ASME Trans. Mechatronics*, vol. 16, no. 4, pp. 768–773, Aug. 2011.
[19] M. Datta, T. Senjyu, A. Yona, T. Funabashi, and C.-H. Kim, "A frequency-control approach by photovoltaic generator in a PV-diesel hybrid power system," *IEEE Trans. Energy Convers.*, vol. 26, no. 2, pp. 559–569, Jun. 2011.
[20] S. G. Li, S. M. Sharkh, F. C. Walsh, and C. N. Zhang, "Energy and battery management of a plug-in series hybrid electric vehicle using fuzzy logic," *IEEE Trans. Veh. Technol.*, vol. 60, no. 8, pp. 3571–3585, Oct. 2011.
[21] U.-C. Moon and K. Y. Lee, "An adaptive dynamic matrix control with fuzzy-interpolated step-response model for a drum-type boiler-turbine system," *IEEE Trans. Energy Convers.*, vol. 26, no. 2, pp. 393–401, Jun. 2011.
[22] A. Elmitwally and M. Rashed, "Flexible operation strategy for an isolated PV-diesel microgrid without energy storage," *IEEE Trans. Energy Convers.*, vol. 26, no. 1, pp. 235–244, Mar. 2011.
[23] A. Payman, S. Pierfederici, and F. Meibody-Taba, "Energy control of supercapacitor/fuel cell hybrid power source," *Energy Convers. Manage.*, vol. 49, no. 6, pp. 1637–1644, Jun. 2008.
[24] P. Thounthong, S. Pierfederici, and B. Davat, "Analysis of differential flatness-based control for a fuel cell hybrid power source," *IEEE Trans. Energy Convers.*, vol. 25, no. 3, pp. 909–920, Sep. 2010.
[25] G. Farivar and B. Asaei, "A new approach for solar module temperature estimation using the simple diode model," *IEEE Trans. Energy Convers.*, vol. 26, no. 4, pp. 1118–1126, Dec. 2011.
[26] P. Lei, Y. Li, and J. E. Seem, "Sequential ESC-based global MPPT control for photovoltaic array with variable shading," *IEEE Trans. Sustain. Energy*, vol. 2, no. 3, pp. 348–358, Jul. 2011.
[27] F.-S. Pai, R.-M. Chao, S. H. Ko, and T.-S. Lee, "Performance evaluation of parabolic prediction to maximum power point tracking for PV array," *IEEE Trans. Sustain. Energy*, vol. 2, no. 1, pp. 60–68, Jan. 2011.
[28] F. Gao, B. Blunier, M. G. Simões, and A. Miraoui, "PEM fuel cell stack modeling for real-time emulation in hardware-in-the-loop applications," *IEEE Trans. Energy Convers.*, vol. 26, no. 1, pp. 184–194, Mar. 2011.
[29] C. Kunusch, P. F. Puleston, M. A. Mayosky, and A. P. Husar, "Control-oriented modeling and experimental validation of a PEMFC generation system," *IEEE Trans. Energy Convers.*, vol. 26, no. 3, pp. 851–861, Sep. 2011.
[30] X.-Z. Yuan, H. Li, S. Zhang, J. Martin, and H. Wang, "A review of polymer electrolyte membrane fuel cell durability test protocols," *J. Power Sources*, vol. 196, no. 22, pp. 9107–9116, Nov. 2011.
[31] X.-Z. Yuan, S. Zhang, J. C. Sun, and H. Wang, "A review of accelerated conditioning for a polymer electrolyte membrane fuel cell," *J. Power Sources*, vol. 196, no. 22, pp. 9097–9106, Nov. 2011.
[32] J. S. Martínez, D. Hissel, M. C. Péra, and M. Amiet, "Practical control structure and energy management of a testbed hybrid electric vehicle," *IEEE Trans. Veh. Technol.*, vol. 60, no. 9, pp. 4139–4151, Nov. 2011.
[33] N. Bizon, "A new topology of fuel cell hybrid power source for efficient operation and high reliability," *J. Power Sources*, vol. 196, no. 6, pp. 3260–3270, Mar. 2011.

Phatiphat Thounthong (M'09) received the B.S. and M.E. degrees in electrical engineering from King Mongkut's Institute of Technology North Bangkok (KMITNB), Bangkok, Thailand, in 1996 and 2001, respectively, and the Ph.D. degree in electrical engineering from Institut National Polytechnique de Lorraine (INPL)-Université de Lorraine, Nancy-Lorraine, France, in 2005.

Currently, he is an Associate Professor in Department of Teacher Training in Electrical Engineering (TE), King Mongkut's University of Technology North Bangkok (KMUTNB). His current research interests include power electronics, electric drives, and electrical devices (FC, PV, wind turbine, batteries, and SC).

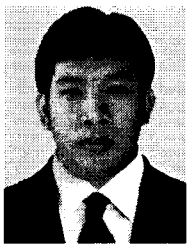

Arkhom Luksanasakul received the B.S. degree in technical education (electrical engineering) from Rajamangala Institute of Technology Nonthaburi Campus, Thailand, in 2000, and received the M.S. degree in technical education (electrical technology) from King Mongkut's Institute of Technology North Bangkok, Thailand, in 2004.

He is currently working toward the Ph.D. degree in electrical education in Department of Teacher Training in Electrical Engineering, King Mongkut's University of Technology North Bangkok, Thailand. His current research interests include engineering education and control system (PID, Fuzzy, Auto-tuning).

Poolsak Koseeyaporn received the B.S. degree in electrical engineering from King Mongkut's Institute of Technology North Bangkok, Thailand, in 1996, and the M.S. and Ph.D. degrees in electrical engineering from Vanderbilt University, Nashville, TN, in 1999 and 2003, respectively.

Currently, he is an Assistant Professor of Electrical Engineering, Department of Teacher Training in electrical engineering, Faculty of Technical Education, King Mongkut's University of Technology North Bangkok (KMUTNB), Thailand. His research interests are control and robotics, engineering, and science learning.

Bernard Davat (M'89) received the Engineer degree from Ecole Nationale Supérieure d'Electrotechnique, d'Electronique, d'Informatique, d'Hydraulique et des Telecommunications (ENSEEIHT), Toulouse, France, in 1975, and the Ph.D. and Docteur d'Etat degrees in elecrical engineering from Institut National Polytechnique de Toulouse (INPT), Toulouse, in 1978 and 1984, respectively.

From 1980 to 1988, he was a Researcher at French National Center for Scientific Research (CNRS), Laboratoire d'Electrotechnique et d'Electronique Industrielle (LEEI). Since 1988, he has been a Professor at Institut National Polytechnique de Lorraine- Université de Lorraine, Nancy-Lorraine, France. His current research interests include power electronics, drives, and new electrical devices (fuel cell and supercapacitor).